52

53

54

55

57

# Self-Consistent Charge Equilibration Method and Its Application to $Au_{13}Na_n$ (n=1,10) Clusters

## Min Zhang† and René Fournier\*,‡

Department of Physics & Astronomy, and Department of Chemistry, York University, Toronto, Ontario, Canada M3J 1P3

Received: July 17, 2008; Revised Manuscript Received: November 28, 2008

We modified the charge equilibration method (QEq) of Rappé et al. by including the third and fourth order terms in the series expansion for the energy of charged atoms. This leads to a self-consistent scheme for obtaining charges and total energy in a molecule. We combined the modified QEq with a scaled morse potential (SMP) to get a new potential, SMP/QEq. The SMP/QEq method allows to do realistic geometry optimizations and calculate reliable charge distributions and ionization energies. The performance of SMP/QEq was fully tested by comparing to high level theories and experiments. We established a connection between first-principles DFT and SMP/QEq which gives insight into SMP/QEq and suggests ways to improve it.

#### I. Introduction

10 11

12

14

15

16

17

18

19

20

23

24

25 26

27

28

29 30

31

32

33

34

35

36

37

39

40

41

42

43

45

48

49

50

Potential functions play a determining role in any molecular simulation. It is important that a potential can estimate charge distribution correctly because not only electrostatic energy is a major part of the cohesive energy, but also charge distribution is crucial to understanding many physical properties, such as molecular reactivity. In the first application of the method that is described here, we showed that different and nontrivial types of AB ordering are possible in  $A_xB_{55-x}$  (A,B = Cu, Ag, Au) clusters depending on differences in electronegativity of the elements and the resulting charge transfer and electrostatic contributions to energy. Many models have been proposed to describe charge distributions in molecules. Some models assign fixed charges to each atom, such as RESP.<sup>2</sup> However, a charge distribution model should depend on the molecular structures or else can treat only structures in close vicinity of the equilibrium geometries that are used to fit parameters of the model. Many methods were developed to estimate the charge distribution dynamically based on the electronegativity equalization principle of Sanderson.<sup>3,4</sup> Examples are the electronegativity equalization method (EEM),<sup>5-8</sup> chemical potential equalization (CPE),9 and charge equilibration (QEq).13 In this study, we modified Rappé's QEq method and combined it with the scaled morse potential (SMP).<sup>1,12</sup> We call this combination SMP/QEq and will explain it in some detail in section IV.

Initially, we implemented QEq based on Rappé's work, <sup>13</sup> but we got some physically unreasonable results. For example, for one of  $Ag_5Li_5$  isomers in Figure 3, QEq assigns a charge bigger than +3 to a Li atom. Rappé et al. mentioned this problem and proposed to fix it by restricting charges to certain reasonable ranges. We believed that two factors contribute to this problem. First, in the original QEq method, the electronegativity  $\chi$  and hardness  $\eta$  are those of the isolated atoms but they are applied to atoms-in-molecule (AIM). <sup>29,30</sup> We suggest instead to obtain a more suitable set of parameters by calculating  $\chi$  and  $\eta$  for AIMs. Second, hardness represents an atom's ability to resist changes to its charge state. But if we charge an atom, both its

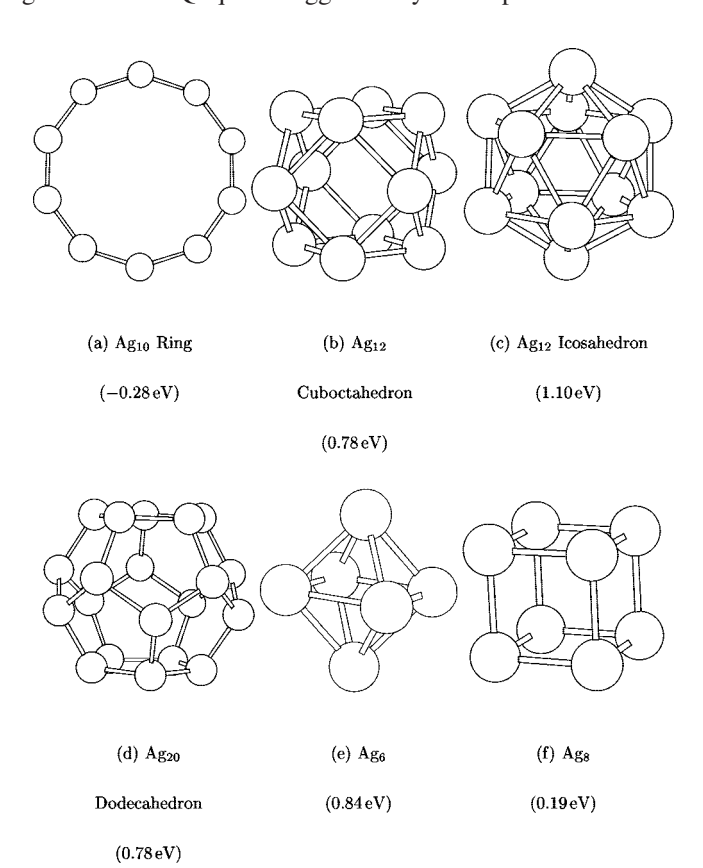


**Figure 1.** Special structures used for fitting. The difference between the first IE from QEq and SVWN,  $\rm IE_{QEq}-\rm IE_{SVWN}$ , are shown in parentheses.

electronegativity and hardness will change. As an extreme example, the hardness of Li<sup>+</sup> is clearly much larger than that of Li. So having a charge dependent hardness could prevent excessive charge build-up. Based on these two points, we developed the model described in the next section.

#### II. Self-Consistent QEq Model

We formulate QEq by expanding atomic energy with respect to charge into a power series and retaining terms up to the fourth

<sup>\*</sup> To whom correspondence should be addressed. E-mail: renef@yorku.ca.

<sup>†</sup> Department of Physics & Astronomy.

<sup>&</sup>lt;sup>‡</sup> Department of Chemistry.

## **B** J. Phys. Chem. A, Vol. xxx, No. xx, XXXX

59

60

61

62

63

65

68

69

70

order instead of the second order as in the original implementation. All of the following discussions are about AIM unless specifically noted. We choose to cut at the fourth order term after trying a few models in the fitting procedure described in section III. This agrees with the suggestion from Iczkowski and Margrave.  $^{16}$  So for atom i we have

$$E_{i}(Q_{i}) = E_{i}(0) + \chi_{i}^{0}Q_{i} + \eta_{i}^{0}Q_{i}^{2} + \frac{1}{6} \left(\frac{\partial^{3}E_{i}}{\partial Q_{i}^{3}}\right) Q_{i}^{3} + \frac{1}{24} \left(\frac{\partial^{4}E_{i}}{\partial Q_{i}^{4}}\right) Q_{i}^{4}$$
(1)

Then by taking the sum of the charge induced energy on all atoms and adding the Coulomb interactions, we will have the total ionic energy of the entire molecule.

$$E(Q_{1},...,Q_{N}) = \sum_{i=1}^{N} [E_{i}(0) + \chi_{i}^{0}Q_{i} + \eta_{i}^{0}Q_{i}^{2} + \frac{1}{6} \left(\frac{\partial^{3}E_{i}}{\partial Q_{i}^{3}}\right) Q_{i}^{3} + \frac{1}{24} \left(\frac{\partial^{4}E_{i}}{\partial Q_{i}^{4}}\right) Q_{i}^{4}] + \sum_{\substack{i>j\\i,j=1...N}} J_{ij}Q_{i}Q_{j} (2)$$

The derivation here is the same as the one in Rappé and Goddard's work.<sup>13</sup> If we take the first derivative of the total electrostatic energy with respect to  $Q_i$ , we have

$$\chi_i(Q_i) = \chi_i^0 + 2Q_i\lambda_i(Q_i) + \sum_{\substack{j \neq i \\ i=1,\dots,N}} J_{ij}Q_j$$
 (3)

Zhang and Fournier

72

73

74

75

77

78

79

80

82

83

where  $\lambda_i(Q_i) = \eta_i^0 + {}^1/_4[(\partial^3 E_i)/(\partial Q_i^3)]Q_i + {}^1/_{12}[(\partial^4 E_i)/(\partial Q_i^4)]Q_i^2$  can be regarded as a charge-dependent hardness,  $J_{ij}$  stands for the screened Coulomb interaction, and  $\chi_i(Q_i)$  is the electronegativity of atom i in the molecule. This modification of QEq requires an iterative calculation because of the nonlinear relation it brings. An iterative scheme was introduced in previous work  $^{14,15}$  but only for the hydrogen atom.

The Sanderson's principle<sup>3,4</sup> states that only one global electronegativity exists in a *N*-atom system. Therefore, when atoms form a molecule, their electronegativities must equalize. For a *N*-atom system, we have

$$\chi_1 = \chi_2 = \dots = \chi_N \tag{4}$$

We also know the total charge on a system

$$Q_{\text{total}} = \sum_{i=1}^{N} Q_i \tag{5}$$

By combining eqs 3-5, we have the linear system

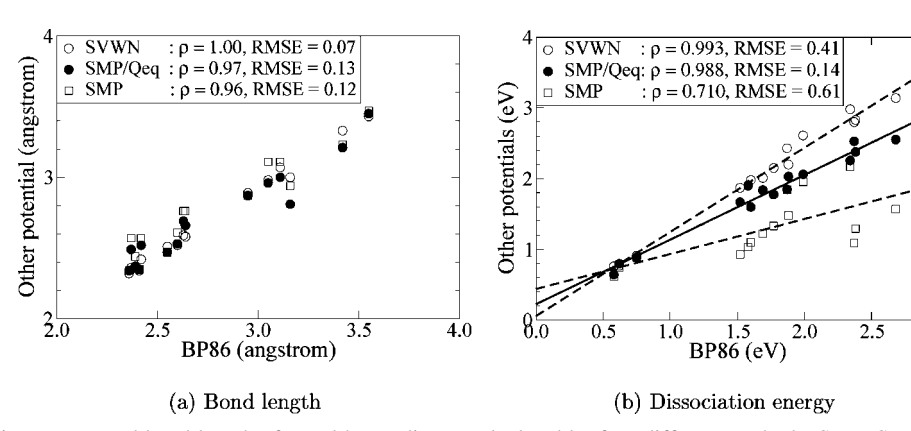


**Figure 2.** Dissociation energy and bond length of metal heterodimers calculated by four different methods, SMP, SMP/QEq, SVWN, and BP86;  $\rho$  and RMSE represent the correlation coefficient and root-mean-square-error, respectively.

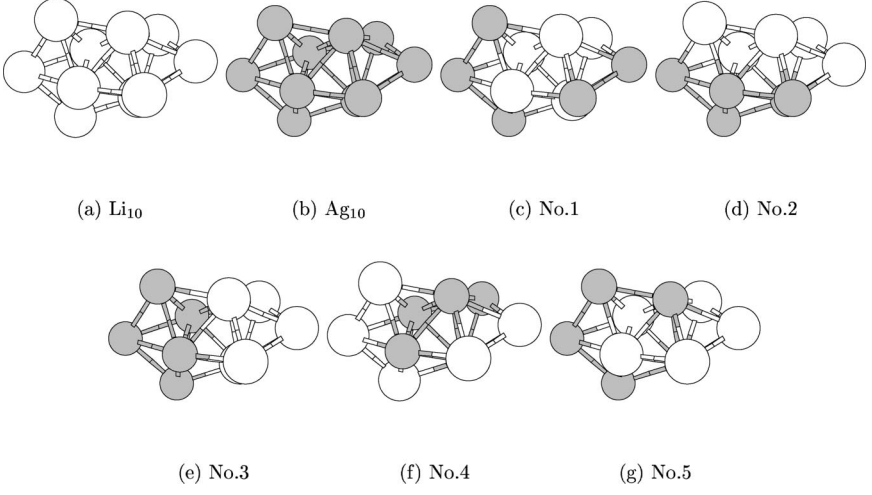


Figure 3.  $Ag_nLi_{10-n}$  (n = 0, 5, and 10) homotops obtained by exchanging the positions of silver and lithium atoms based on the same geometry. Lithium atoms are in white.

124

126

127

128

129

130

131

132

133

134

135

136

137

138

139

140

141

142

143

144

145

146

147

148

149

150

151

152

153

154

155

156

157

158

159

160

161

162

163

164

165

166

167

168

$$\begin{bmatrix} J_{21} - J_{11} & J_{22} - J_{12} & J_{23} - J_{13} & \dots & J_{2i} - J_{1i} & \dots & J_{2N} - J_{1N} \\ J_{31} - J_{11} & J_{32} - J_{12} & J_{33} - J_{13} & \dots & J_{3i} - J_{1i} & \dots & J_{3N} - J_{1N} \\ \vdots & \vdots \\ J_{i1} - J_{11} & J_{i2} - J_{12} & J_{i3} - J_{13} & \dots & J_{ii} - J_{1i} & \dots & J_{iN} - J_{1N} \\ \vdots & \vdots & \vdots & \vdots & \vdots & \vdots & \vdots \\ J_{N1} - J_{11} & J_{N2} - J_{12} & J_{N3} - J_{13} & \dots & J_{Ni} - J_{1i} & \dots & J_{NN} - J_{1N} \end{bmatrix} \times \\ \begin{bmatrix} Q_1 \\ Q_2 \\ \vdots \\ Q_i \\ \vdots \\ Q_{i-1} \\ Q_{i-1}$$

For  $J_{ij}$ , if  $i \neq j$ , we use the empirical function developed by Louwen and Vogt.<sup>10</sup>

$$J_{ij} = \left(\frac{1}{\gamma_{ij}^{3}} + R_{ij}^{3}\right)^{-1/3} \tag{7}$$

where  $\gamma_{ij} = 2[\eta_i^0 \eta_j^0]^{1/2}$ . When i is equal to j, we have  $J_{ii} = 2\lambda_i(Q_i)$ , which is a charge dependent parameter. In eqs 6 and 7, all quantities are in atomic units. To develop the linear system, we rewrite eq 4 to N-1 equations,  $\chi_i - \chi_1 = 0$ , where i = 2,...,N This choice is arbitray and assigns a "special status" to atom 1 in the linear system. But this should not cause any problem when we apply the LU decomposition with partial pivoting and row interchanges to solve the linear system, and in practice, we have not encountered any case of numerical instability.

### **III. Fitting Procedure**

84

85

86

87

88

89

90

91

94

95

96

97

98

100

101

102

103

104

105

106

107

108

109

110

111

112

113

114

115

116

117

118

119

120

121

122

The major difficulty in implementing this scheme is that the various energy derivatives in eq 1, including  $\chi_i^0$  and  $\eta_i^0$ , are unknown. We designed a fitting procedure to obtain them from a higher level theory, in the present work density functional theory (DFT) in the local spin density approximation with a "SVWN" exchange-correlation functional.<sup>20–23</sup> For fitting, we selected model structures in which all atoms are equivalent, as shown in Figure 1. The simplest one is a 10-atom ring. We found that when a ring contains more than 10 metal atoms DFT calculations are costly and very hard to convergence. On the other hand, smaller rings give less data for fitting and bigger error could arise due to atomic interactions between nonneighbor atoms that are closer to each other. Other highsymmetry structures can be used such as 12-atom cuboctahedron, 12-atom icosahedron, 20-atom dodecahedron, etc. We chose these high-symmetry structures because the partial charge on each atom can be simply calculated by  $Q_i = Q_{\text{total}}/N$ , so we do not have to choose among different charge decomposition schemes in ab initio calculations. Another benefit is that coefficients are always identical for all atoms in a model system and this simplifies our fitting procedure. The fitting procedure consists of the following steps. First, for a N-atom structure, we calculate the total energies with different charges,  $E_{\text{total}}(Q_{\text{total}})$ , where  $Q_{\text{total}}$  ranges from -1 to N, using SVWN/DFT and the deMon software.33 Spin states were restricted to singlet or doublet. Model core potentials were used for Ag and Au, with

**TABLE 1:** Coefficients of the E(Q) Polynomial Fit

element	first	second	third	fourth	χ	λ	$2nd/\lambda$
Li	3.0215	3.2426	0.9056	0.0566	3.01	2.39	1.357
Na	2.8815	3.1339	0.6762	-0.1326	2.85	2.30	1.362
K	2.4419	2.5684	0.5326	-0.0996	2.42	1.92	1.337
Rb	2.3138	2.4580	0.5036	-0.1247	2.33	1.85	1.329
Cu	5.2775	4.1921	0.3808	0.2151	4.48	3.25	1.290
Ag	5.1362	4.2742	0.4097	-0.0490	4.44	3.14	1.361
Au	6.3450	4.0789	0.1825	0.1245	5.77	3.46	1.179
Al	3.8002	2.7974	0.1283	0.7036	3.21	2.78	1.006

17 electrons per atom being treated explicitly. All electron treatments were done for the other elements. The basis sets were of double- $\zeta$  quality (except triple- $\zeta$  for K) with diffuse and polarization functions for all elements except Ag and Au. The auxiliary basis sets were standard ones used in the deMon software.<sup>33,34</sup> From each calculation we can extract a pair of data, charge on each atom and corresponding atomic charge-induced energy,  $(Q_i, E_i(Q_i))$ . As mentioned earlier,  $Q_i$  is simply equal to  $Q_{\text{total}}/N$  due to symmetry. We get the AIM charging energy as

$$E_{i}(Q_{i}) = [E_{\text{total}}(Q_{\text{total}}) - E_{\text{total}}(0) - \sum_{\substack{m < n \\ m, n = 1 \cdots N}} J_{mn}Q_{m}Q_{n}]/N$$
(8)

The right-hand side of eq 8 could be interpreted as follows. we use the neutral system as the reference for energy and subtract it from the energy of the charged systems. The underlying assumption in eq 8 is that the nonionic terms in the energy are equal in the neutral and charged systems. Therefore, the energy difference between neutral and charged has two contributions: (i) the energy for charging atoms and (ii) the pairwise electrostatic interactions between atoms. After we subtract Coulomb energies, represented by the sum term in eq 8, we have only the energy for charging atoms left. Again because of symmetry we can obtain  $E_i(Q_i)$  simply by dividing the total charge-induced energy by N. In fitting, we approximate  $J_{ii}$  by eq 7. In this procedure, we must choose sensible interatomic distances. After many trials we decided that the best choice is simply to set the nearest neighbor distance  $(d_{NN})$  in the model system equal to  $d_{\rm NN}$  of the corresponding bulk system. The fitting results from different model structures are not identical. We expect this difference since atoms in different model systems are in distinct molecular environment, strictly they are different AIMs, and this should be reflected in the parameters obtained. Ideally, we should choose parameters from model systems resembling the dominant cluster structures which are usually compact and have high coordination numbers. However, we compared the performance of SMP/QEq using different sets of coefficients, and found that those from the simplest model structure (10-atom ring) work the best. We elaborate on this point in section V.B. A possible reason is that in our fitting precedure we introduced a few approximations. The more complex a structure is, the bigger the error is from approximations due to the entanglement of its atomic interactions. The 10-atom ring has the simplest structure and the lowest coordination. The only negative point of a 10-atom ring is that it does not possess a compact structure typical of low energy clusters structures. This defect causes a systematic error that will be discussed in section VD.

The coefficients we obtained with this fitting procedure for eight metals are listed in the first four columns of Table 1. Since

## **D** J. Phys. Chem. A, Vol. xxx, No. xx, XXXX

170

171

172

173

174

175

176

177

178

179

180

181

183

184

185

186

187

188

189

190

191

192

193

194

195 196

197

198

199

200

201

202

203

we use neutral systems as reference for energy, as expected, the zeroth order coefficients are essentially zero. In the next two columns of the table, we list the electronegativity  $\chi$  and hardness  $\lambda$  of isolated atoms from Parr and Yang's book, <sup>17</sup> which are counterparts to the first and second order coefficients. The last column contains the ratio of our hardness to theirs. We observe that for alkali we obtained almost the same electronegativity and bigger hardness. For group 11 elements, both electronegativity and hardness are bigger than Parr and Yang's values. For Al we obtained a bigger electronegativity but the same hardness. The second order coefficients are almost always bigger than those from Parr and Yang's book, meaning atoms in molecules are harder than the isolated ones. Consequently, unphysical big charges generated by using parameters for isolated atoms will be reduced if we apply those found for atoms in molecules. In addition, the third and fourth parameters give a more realistic description of systems with large atomic charges.

## IV. Explanation of SMP/QEq by DFT

We now wish to review some aspects of DFT formalism<sup>17</sup> in order to show the assumptions that give rise to SMP/QEq and similar approximate methods.

Consider a N-electron system: if the external potential v(r) is known, the Hamiltonian of the system is determined. Thus N and v(r) determine all ground-state properties of the system. The derivatives of energy with respect to N and v(r) are

$$\mu = \left(\frac{\partial E}{\partial N}\right)_v \tag{9}$$

$$\eta = \frac{1}{2} \left( \frac{\partial \mu}{\partial N} \right)_v = \frac{1}{2} \left( \frac{\partial^2 E}{\partial N^2} \right)_v \tag{10}$$

$$f(r) = \left(\frac{\delta\mu}{\delta v}\right)_{N} = \left(\frac{\partial\rho(r)}{\partial N}\right)_{v} \tag{11}$$

$$\rho(r) = \left[ \frac{\delta E}{\delta v(r)} \right]_{N} \tag{12}$$

In these relations,  $\mu$  is the chemical potential of the system,  $\eta$  is the absolute hardness, f(r) is the Fukui function, and  $\rho(r)$  is the ground-state electron density. With the help of these derivatives, we can do a Taylor expansion for the ground-state energy (see ref 17, page 226)

$$\Delta E = \mu^{0} \Delta N + \eta^{0} (\Delta N)^{2} + \Delta N \int f^{0}(r) \Delta v(r) dr + \frac{1}{2} \int \int \left[ \frac{\delta \rho^{0}(r)}{\delta v(r')} \right]_{N} \Delta v(r) \Delta v(r') dr dr' + \int \rho^{0}(r) \Delta v(r) dr$$
(13)

where we use superscript "0" to indicate quantities for the system before any changes. Since electronegativity  $\chi$  is equal to  $-\mu$  and charge Q is equal to  $-\Delta N$ , we can substitute variables in eq 13 and get

$$\Delta E = \chi^0 Q + \eta^0 Q^2 - Q \int f^0(r) \Delta v(r) dr + \frac{1}{2} \int \int \left[ \frac{\delta \rho^0(r)}{\delta v(r')} \right]_N \Delta v(r) \Delta v(r') dr dr' + \int \rho^0(r) \Delta v(r) dr (14)$$

If only the external potential v(r) changes, the first, second, and third terms in eq 14 will be zero. If v(r) is fixed and N varies, the fourth, fifth, and third terms will disappear. So we can say, in regard to energy, that the first and second terms describe the effect of varying the number of electrons and the

describe the effect of varying the number of electrons and the fourth and fifth terms tell us how changes of external potential induce energy variation. The third term shows the compound

effect when both quantities are changed.

Let us consider our simplest model system, a 10-atom ring, Figure 1a. From the viewpoint of atom i, other atoms serve as particle source and additional external field. We use eq 14 to represent the energy change,  $\Delta E_i$ , for atom i when forming a ring. If the ring is neutral, because all atoms are equivalent, every atom has a zero charge. This means terms 1, 2, and 3 will be zero. Because bonding changes  $v_i(r_i)$ , terms 4 and 5 will not be zero and their sum is  $\Delta E_i$ . This is what SMP attempts to represent. That is, in SMP/QEq we use SMP<sup>1,12</sup> to approximate terms 4 and 5 in eq 14 due to nonionic interaction. The only conceptual difference is that SMP assigns energy to bonds, but terms 4 and 5 in eq 14 assign the same energy to atoms. Actually, other potentials, such as embedded-atom method (EAM)<sup>31</sup> and Morse potential,<sup>32</sup> can do the same thing. It is essential, however, that the chosen empirical potential be "purely covalent", i.e., that it does not attempt in any way to describe ionic or other electrostatic interactions. The SMP fits this criterion perfectly.

Now let us change the energy further by charging the ring while keeping its size fixed.  $\chi^0$  and  $\eta^0$  were changed during ring formation. To avoid any ambiguity, we rewrite eq 14 as

$$\Delta E_{i} = \chi_{2i}^{0} Q_{i} + \eta_{2i}^{0} Q_{i}^{2} - Q_{i} \int f_{2i}^{0}(r_{i}) \Delta v(r_{i}) dr_{i} + \frac{1}{2} \int \int \left[ \frac{\delta \rho_{2i}^{0}(r_{i})}{\delta v_{i}(r'_{i})} \right]_{N} \Delta v(r_{i}) \Delta v(r'_{i}) dr_{i} dr'_{i} + \int \rho_{2i}^{0}(r_{i}) \Delta v(r_{i}) dr_{i}$$
(15)

The subscript 2 represents coordination number and serves as a reminder that the parameters refer to an AIM not an isolated atom. For atom i,  $\Delta E_i$  comes from two sources, charge  $Q_i$  and  $\Delta v_i(r_i)$  We need to make a few approximations to reach the main equation of QEq. First, we approximate  $\Delta v_i(r_i)$  by the Coulomb field generated by charges on other atoms. We also accept the "frozen core" assumption. Under this assumption, when an atom gains negative charges, the only change to its density is that additional electron density is added to its lowest unoccupied molecular orbital (LUMO). Similarly, the only change to a positively charged atom is that the positive charge spreads in its highest occupied molecular orbital (HOMO). So we can approximate atom i's contribution to  $\Delta v_i(r_i)$  as  $g_i(r_i) =$  $-Q_i \int (\rho_i(r_i))/(|r_i-r_i|) dr_i$  where  $\rho_i(r_i)$  is the density of the LUMO or HOMO of atom j, depending on the sign of  $Q_j$  Then we have  $\Delta v_i(r_i) = \sum_{i \neq i} g_i(r_i)$  Usually,  $f^0(r)$  is approximated using central difference as:  $f^0(r) \approx \frac{1}{2} [\rho_{\text{LUMO}}(r) + \rho_{\text{HOMO}}(r)]$  [ref 17, p 99]. Here we choose a one-sided difference formula and get  $f^{0}(r) \approx \rho_{i}(r_{i})$ , where  $\rho_{i}(r_{i})$  is the density of LUMO or HOMO depending on the sign of  $Q_i$  We can rewrite the third term in eq 15 as

205

206

207

Zhang and Fournier

214

227

228229230231

231 232

234

251 252 253

255

257

258

259

260

261

262

263

264

265

266

267

268

269

270

271

272

273

274

275

276

279

280

281

282

283

285

286

287

288

291

292

293

294

295

296

297

298

299

300

302

303

304

305

306

307

308

309

310

311

313

314

315

316

317

318

319

320

321

322

323

324

325

326

327

328

329

331

332

333

334 335

336

337

338

339

340

341

342

343

344

345

346

347

348

350

351

352

$$-Q_{i} \int f_{2i}^{0}(r_{i}) \Delta v(r_{i}) dr_{i} \approx Q_{i} \sum_{j \neq i} \int \int \frac{Q_{j} \rho_{i}(r_{i}) \rho_{j}(r_{j})}{|r_{i} - r_{j}|} dr_{i} dr_{j} = \sum_{\substack{j \neq i \\ j = 1 \cdots N}} J_{ij} Q_{i} Q_{j}$$
 (16)

Another approximation is that we neglect terms 4 and 5 in eq 15 if we believe that the disturbance to external field due to Coulomb field contributes little to energy change via terms 4 and 5 compared to other terms. Accepting this simplification, we in fact represent terms 4 and 5 by SMP completely. After all these approximations, we get the equation

$$\Delta E_{i} = \chi_{2i}^{0} Q_{i} + \eta_{2i}^{0} Q_{i}^{2} + \sum_{\substack{j \neq i \\ j=1 \cdots N}} Q_{i} Q_{j} J_{ij}$$
 (17)

 $\Delta E_i$  represents the ionic energy of atom i if we treat other atoms as particle source and additional external field. This way of thinking makes us assign all of the Coulomb energy between atom i and all other atoms to atom i as potential energy. That is, considering atom i and j, when we write down eq 17 for atom i, the Coulomb energy between these two atoms is completely given to atom i. In eq 17 for atom j, we assign this energy to atom j. So when we sum ionic energies represented by eq 17 to get total ionic energy, we have to avoid double counting of Coulomb energies

$$\Delta E_{\text{total}}(Q_1, ..., Q_N) = \sum_{i=1}^{N} (\chi_{n_i i}^0 Q_i + \eta_{n_i i}^0 Q_i^2) + \sum_{\substack{i > j \\ i, j = 1 \cdots N}} Q_i Q_j J_{ij}$$
 (18)

In eq 18, the subscript  $n_i$  represents the environment around atom i since eq 17 is true for any AIM. If we take the first derivative of  $\Delta E_{\text{total}}$  with respect to  $Q_i$ , we have the basic equation of QEq.<sup>13</sup> Adding higher order terms to the equation above will give

$$\chi_{i}(Q_{i}) = \chi_{n_{i}i}^{0} + 2Q_{i}\lambda_{n_{i}i}(Q_{i}) + \sum_{\substack{j \neq i \\ j=1 \dots N}} J_{ij}Q_{j}$$
 (19)

where  $\lambda_{n,i}(Q_i) = \eta_{n,i}^0 + \frac{1}{4}[(\partial^3 E_i)/(\partial Q_i^3)]_{n,i}^0 Q_i + \frac{1}{12}[(\partial^4 E_i)/(\partial Q_i^4)]_{n,i}^0 Q_i^2$ . This the basic equation in our version of QEq, eq 3. If we apply eq 19 to all of our model systems, the only difference is the subscripts representing molecular environment,  $n_i$ . That is to say, when we perform fitting using different model systems, we will get parameters for different AIMs.

### V. Result

To test the performance of SMP/QEq, we did several calculations. Results are shown and discussed below.

**A. Diatomic Molecules.** Metal heterodimers are the simplest alloy systems. In this test, we calculated the bond length,  $R_e$ , and dissociation energy,  $D_e$ , for 15 heterodimers AB (A,B = Li, Na, K, Cu, Ag, and Au). Four different methods, SMP, SMP/QEq, SVWN, and BP86,  $^{26,27}$  were used. Results are summarized in Figure 2. We use results from BP86 as a reference because

it is theoretically the best method and also because it generally agrees with experiment better than SVWN. The other methods are compared to BP86. Figure 2b shows comparison for  $D_{\rm e}$ . The points gathered around 0.6 eV are for LiNa, LiK, and NaK in which ionic interaction is weak since Li, Na, and K have similar electronegativities. In those three cases, SMP and SMP/ QEq give almost the same values as SVWN and BP86, as expected. However, things are quite different when ionic interaction plays an important role as shown by the rest of the graph. Overall, data from SVWN and BP86 are highly correlated with a correlation coefficient of 0.993. On the contrary, SMP gives us the least correlated results with respect to those of BP86. The correlation coefficient is only 0.710, and the slope is off that of SVWN by a lot. By adding the QEq components, we not only improved the correlation coefficient to 0.988, but also bring the slope much more closer to that from SVWN results. Looking at the root-mean-square-errors (RMSE) in Figure 2b, we see that the SMP/QEq dissociation energies are much more consistent with BP86 results than those from the other methods. So we can say that the ionic interaction is essential to calculate  $D_e$  of heterodimers and that QEq estimates it well. Surprisingly, as shown in Figure 2a, all potentials give similar results for bond length. This is because the energy curve for ionic interaction has a small slope near the minimum of the nonionic energy curve, so adding the ionic component changes the depth of the energy curve a lot but does not affect the minimum position much.

B. Li and Ag Alloy Clusters. An advantage of SMP/QEq over most empirical potentials is that it includes a crude model of electronic structure and can be used to evaluate ionization energy (IE). In this section, we compared IE calculated with SMP/QEq and with higher level theories, SVWN, B3LYP, <sup>24,25</sup> and BP86. Our sample systems, shown in Figure 3, include five homotops of Ag<sub>5</sub>Li<sub>5</sub>, which are all based on the same geometry but with different site occupation by the two elements, and pure clusters Ag<sub>10</sub> and Li<sub>10</sub>. We calculated the first and second IEs and plotted results in Figure 4, panels a and b. Note that for structure no. 5 we were unable to get BP86 results because of SCF convergence problems. SMP/QEq results follow the trend of values from SVWN well but are consistently higher. On average, SMP/QEq overestimated the first IE by 0.61 eV comparing to SVWN, and the overestimation is 1.10 for the second IE. It is quite encouraging that SMP/QEq successfully describes the relative values of IEs, but the systematic overestimation is puzzling. We will go back to this question in section

As we said in section III, the parameters obtained from the 10-atom ring are better than those from other model systems. This can be seen by looking at the first IE of the Li<sub>5</sub>Ag<sub>5</sub> homotops in Figure 3. Using the 12-atom icosahedron parameters, QEq failed to give physically meaningful results for homotops nos. 3, 4, and 5. The IEs calculated for the homotops in Figure 3 are, in order from (a) to (g): 3.98, 6.09, 5.59, 4.71, 4.26, 4.37, and 4.76 eV with the 12-atom cuboctahedron parameters and 4.07, 6.57, 5.63, 4.95, 4.73, 4.59, and 5.01 eV with the 20-atom dodecahedron parameters. Overall, linear regressions show that IEs based on the parameters from the 10atom ring correlate well with those from SVWN with a correlation coefficient of 0.994, whereas the correlation coefficient is 0.95 for the 20-atom dodecahedron model, and 0.92 for the 12-atom cuboctahedron model. The difference of IE between nos. 3 and 2, and between nos. 3 and 4, is particularly instructive: SVWN (the reference) gives +0.14 and +0.77 eV; other DFT functionals give results similar to SVWN; QEq

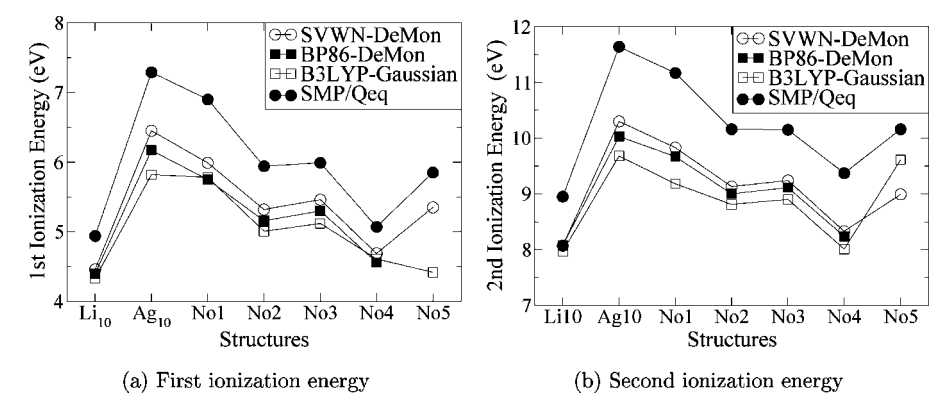
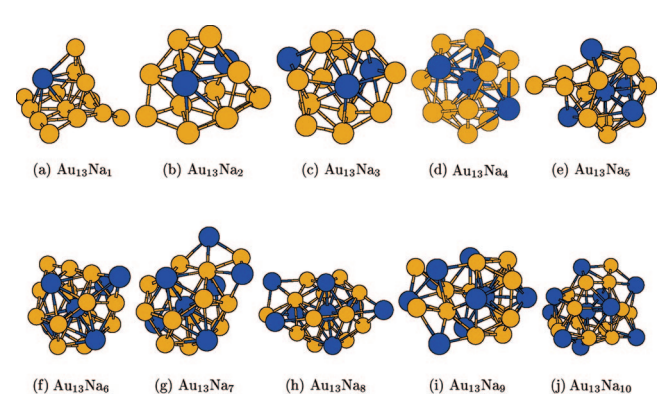


Figure 4. First and second ionization energy of  $Ag_nLi_{10-n}$  (n=0, 5, and 10) isomers shown in Figure 3.



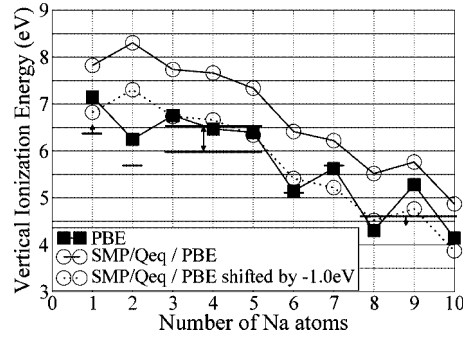
**Figure 5.** Global minimum of  $Au_{13}Na_n$  (n = 1-10) clusters obtained by TSDS with VASP/PBE.

TABLE 2: Mixing and Cage-Like Indices of  $Au_{13}Na_x$  (x = 1-13) Clusters

X	OMI	LMI	CLI
1	0.179	0.031	0.34
2	0.732	0.052	0.56
3	0.838	0.078	0.64
4	0.768	0.062	0.39
5	0.938	0.056	0.43
6	0.866	0.056	0.40
7	0.898	0.077	0.38
8	0.886	0.081	0.39
9	0.888	0.092	0.49
10	0.976	0.111	0.53

parametrized with the 12-atom cuboctahedron gives -0.46 and -0.11 eV; QEq parametrized with the 20-atom dodecahedron gives +0.13 and -0.22 eV; and QEq parametrized with the 10-atom ring gives +0.04 and +0.94 eV. Note also that IEs calculated from QEq are lower when the model structures have higher coordination numbers.

**C. Au and Na Alloy Clusters.** We performed further test on SMP/QEq's ability to estimate ionization energy because, in our previous test, the sample size is small, only Ag and Li are involved, and we only compared to other theory. Nakajima et al. 19 measured the first IE of  $Au_{13}Na_n$ , n = 1,10. In order to compare to experiment, we need to find out the structures of these clusters. We did global optimizations by tabu search in descriptor space (TSDS) 18 method. The PBE 18 functional implemented in VASP was used to evaluate energies for optimizations. The global minima (GM) are shown in Figure 5. Three quantities are calculated to show their structural characters and are listed in Table 2. The first one is an overall mixing index (OMI) which represents the mixing of two elements on a large scale. The second one is a local mixing index (LMI) which shows how two elements are mixed locally.



**Figure 6.** Vertical ionization energy of  $Au_{13}Na_n$  (n = 1-10) clusters shown in Figure 5.

The last quantity is a cage-like index (CLI) which is a measure we designed to quantify how much a cluster resembles a cage. Mixing indices are of obvious interest in bimetallic clusters. The CLI is of special interest here because cage structures have been proposed for gold clusters ("golden cages") in a size range from 15 to 20 atoms roughly. We will now briefly explain the OMI, LMI, and CLI. Suppose that we have two kinds of elements A and B in a cluster. We use the symbols  $d_{AA}$  and  $d_{BB}$  to represent the nearest-neighbor distances for bulk A and B, respectively. Then  $d_{AB} = (d_{AA} + d_{BB})/2$  is the estimated A–B bond length. We denote by  $\vec{c}_{BA}$  the vector that starts at the center of mass of atoms of B type and ends at the center of mass of atoms of A type: its norm is  $||\vec{c}_{BA}||$  We use  $P_{B_iA_j}$  to represent the projection of the vector from the *i*th atom of type B to the *j*th atom of type A on the direction  $\vec{c}_{BA}$ , so

$$P_{B_i A_j} = (\vec{r}_{A_j} - \vec{r}_{B_i}) \cdot \vec{c}_{BA} / ||\vec{c}_{BA}||$$
 (20)

here  $\vec{r}_{A_j}$  and  $\vec{r}_{B_i}$  are the position vectors of the jth atom of type A and ith atom of type B. By moving all A type atoms together along direction  $\vec{c}_{BA}$  until A and B type atoms are completely separated, we can get the displacement,  $\Delta$ , needed to reach complete separation. Figure 7 gives illustrates this process. Figure 7a is a hypothetical structure; 7b shows what happens to to the position vectors and  $\vec{c}_{BA}$  as atoms of A type and B type are pulled apart ( $\Delta$  is increased); and Figure 7c shows how the projection of vectors  $(\vec{r}_{A_j} - \vec{r}_{B_i})$  on the vector  $\vec{c}_{AB}$  all become positive at some value of  $\Delta$ . Choosing a criterion for complete separation is subjective and depends on a given application. We define that A and B type atoms are completely separated when the relation  $P_{B_iA_j} \geq d_{AB}/4$  is true for all i and j. We define the OMI as

405

406

407

408 409

410

411

412

413

414

415

418

419

420

421

422

423

424

425

426

427

428

429

430

431

432

433

436

437 438

439

440

441 442

443

444

445

446

448

$$OMI = \frac{\Delta}{||\vec{c}_{BA}|| + \Delta}$$
 (21)

To define the LMI, we need three quantities  $\bar{s}_{AA}$ ,  $\bar{s}_{BB}$ , and  $\bar{s}_{AB}$ . The variable  $\bar{s}_{AA}$  is a weighted average of the scaled A-A pair distances

$$\bar{s}_{AA} = \frac{\sum_{i < j} w_{ij} \cdot (||\vec{r}_{A_i} - \vec{r}_{A_j}||/d_{AA})}{w_{ij}}$$
 (22)

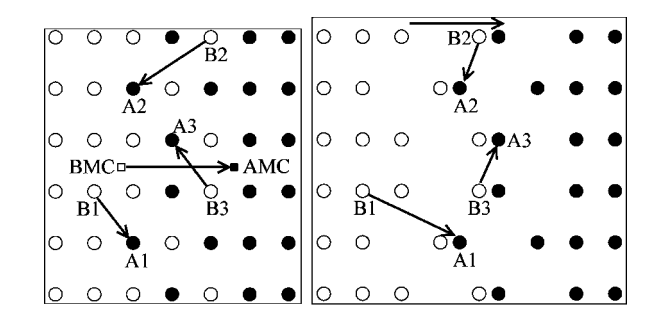
where  $w_{ij} = [(|\vec{r}_{A_i} - \vec{r}_{A_j}|])/d_{AA}]^{-4}$ , and the sum goes over all A-A pairs. The quantities  $\bar{s}_{BB}$  and  $\bar{s}_{AB}$  are defined in a similar way. We choose a negative power of pair distances as weights to emphasize short bonds in the weighted average. But if we put too much weight on short bonds, the weighted average will be determined only by the shortest pair distance. The power -4 is chosen as a compromise Finally, we have this definition for LMI

$$LMI = 1 - \frac{\overline{s}_{AB}}{(a/t)\overline{s}_{AA} + (b/t)\overline{s}_{BB}}$$
 (23)

where a is the number of A-A pairs, b is the number of B-B pairs, and t = a + b. We illustrate the meaning of the OMI and LMI with examples of configurations shown in Figure 8. The OMI for Figure 8a-d are 0, 1, 1, and 0, respectively. For Figure 8, panels a, b, and d, LMI < 0 (poor mixing), and for Figure 8c, LMI > 0 (good mixing) because the AB distances are smaller, on average, than the AA or BB distances. Clearly, case 8a (and 8d) is poorly mixed at any scale, and case 8c is well mixed at any scale. Case 8b is well mixed in a global sense (OMI = 1) but poorly mixed in local sense (LMI < 1). The definition of CLI depends on two quantities which we will now explain. Consider an arbitrary point p in a cluster with position  $\vec{x}_p$ , and denote by  $d_{ip}$  the distance between this point and atom *i* We define the function f of  $\vec{x}_p$ :  $f(\vec{x}_p) = \min\{d_{ip}: \text{ all } i\}$  Let  $d_0$  be the maximum value of  $f(\vec{x}_p)$  among all interior points of the cluster. This  $d_0$  has a geometric interpretation: it is half the length of the longest stick that could be placed at a fixed position in the cluster and could rotate freely in any direction without intersecting any of the nuclei positions. The cube of  $d_0$  (or  $4\pi d_0^3$ / 3) is then a measure of the largest empty space that could be found in the cluster. Another relevant quantity is  $d_{\min}$ , the smallest interatomic distance in the cluster. The cube of  $d_{\min}$  is a way to quantify the volume associated with a missing atom defect in a structure. The CLI is a comparison of these two volumes

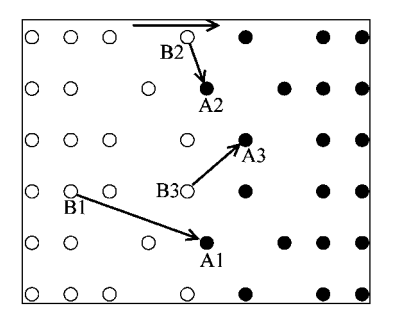
$$CLI = \frac{d_0^3}{d_{\min}^3} \tag{24}$$

Division by  $d_{\min}$  ensures that the same CLI is obtained when a cluster is uniformly expanded. A CLI value greater than one is consistent with this concept of a cage: a continuous empty region of space inside a cluster whose size is clearly bigger than the usual space between atoms. From Table 2, we can observe that all LMIs are smaller than 1. This indicates good local mixing, with  $Au_{13}Na_{10}$  having the highest degree of local mixing. Cluster  $Au_{13}Na_1$  has an OMI close to zero. This is simply because the only Na atom resides on its surface. The values of OMI being



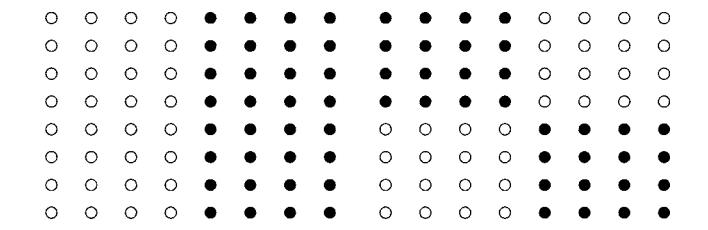
(a) Initial mixed state

(b) Partial separation



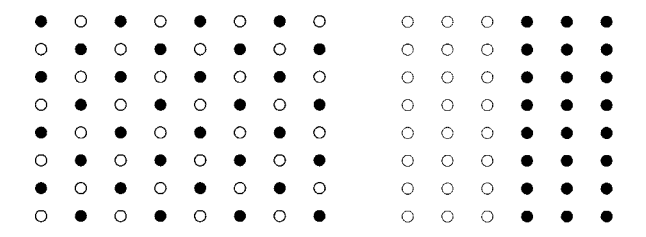
### (c) Complete separation.

**Figure 7.** Illustration of how the OMI is calculated. Atoms of A are shown as filled circles, B as open circles. In (a), BMC and AMC are the centers of mass of B-type atoms and A-type atoms, respectively: the vector connecting them is  $\vec{c}_{AB}$ .



(a) Case 1.

(b) Case 2.



(c) Case 3.

(d) Case 4.

450

451

452

453

**Figure 8.** Four types of AB ordering used to illustrate the OMI and LMI: (a) and (d) no overall mixing and poor local mixing; (b) good overall mixing, poor local mixing; (c) good overall mixing and good local mixing.

close to one for all other clusters tell us that Au and Na atoms are well mixed on a large scale. Clusters Au<sub>13</sub>Na<sub>2</sub> and Au<sub>13</sub>Na<sub>4</sub> have slightly lower OMIs than other clusters except Au<sub>13</sub>Na<sub>1</sub>. By looking at their pictures in Figure 5, we can clearly see that Na atoms really show a tendency to gather on one side of the clusters. Before looking at CLIs of Au<sub>13</sub>Na<sub>n</sub>, we want to mention

457

458

460

461

462

463

464

465

467

468

469

470

471

472

473

474

475

476

477

478

480

481

482

483

484

485

488

489

490

491

492

493

495

496

497

498

499

500

501

503

504

505

506

507

508

509

511

512

513

514

515

516

517

520

521

522

523

525

526

527

529

530

531

532

534

535

536

537

539

540

541

543

544

545

547

548

549

550

552

553

554

555

557

558

559

560

561

562

563

564

566

567

568

569

570

571

572

573

574

575

576

577

578

the CLIs of special structures. The CLIs for the 12-atom cuboctahedron (Figure 1b), 12-atom icosahedron (Figure 1c), and 20-atom dodecahedron (Figure 1d) are 1.00, 0.86, and 2.75, respectively. These values are typical of true cages. The CLI of the icosahedron being smaller than 1 reflects the fact that the central atom in a 13-atom icosahedron is slightly compressed. On the other hand, compact structures with no cage feature at all have CLI values in the vicinity of 0.246 (13-atom icosahedron) or 0.230 (13-atom cuboctahedron). If we take the criterion that the 12-atom icosahedron is the smallest possible cage, then structures with CLI smaller than 0.86 are not truly cages. The CLIs in Table 2 show that none of our Au/Na alloy clusters has a cage. Among all clusters, Au<sub>13</sub>Na<sub>2</sub>, Au<sub>13</sub>Na<sub>3</sub>, and Au<sub>13</sub>Na<sub>10</sub> have relatively large CLIs. Figure 5, panels b and c, shows us clearly that Au<sub>13</sub>Na<sub>2</sub> and Au<sub>13</sub>Na<sub>3</sub> do have empty space inside but are simply not large enough to accommodate an atom of a size comparable to a gold atom. It is not easy to visualize empty space in Au<sub>13</sub>Na<sub>10</sub> shown in Figure 5j, but when we look closely we see that a part of the cluster is open.

Based on these structures, the first IEs were calculated by SMP/QEq and PBE. Results together with experimental values are shown in Figure 6. The experimental values or ranges are shown by horizontal bars with arrows. The PBE results fall close to experiment except for Au<sub>13</sub>Na<sub>2</sub> and Au<sub>13</sub>Na<sub>9</sub>. There are many possible factors that may explain these two mismatches. In experiment, the measurement could relate to isomers other than the GM, so the IE may be an average of different isomers. It is also possible that our global optimization did not reach the true GM. It is an embarrassment in any global optimization that one never knows that the GM was obtained. All we can say is that these structures are the best we could get. Based on the results for these 10 clusters, we still can say that our global optimization generated sensible results and IEs calculated by PBE resemble the experiment. SMP/QEq again gives results consistently higher than those of PBE and experiment. The average overestimation is 1.0 eV as before. If we shift down the SMP/QEq curve by 1.0 eV to make comparison easier (dashed lines in Figure 6), we see that SMP/QEq results agree well with those from PBE and experiments except for Au<sub>13</sub>Na<sub>2</sub> and Au<sub>13</sub>Na<sub>7</sub>. There are plenty of possible error sources, particularly the fact that SMP/ QEq does not include any quantum effects which could be important for structures with a magic number of electrons (20) like Au<sub>13</sub>Na<sub>7</sub>. Adding a correction for electronic shell closing into SMP/QEq might improve it. Another important error source is that our parameters were fitted based on a ring structure which is different from the compact structures of most metal clusters.

**D. Systematic Error.** As shown in the previous two sections, systematic errors persist in ionization energy calculations. From the fitting precedure described in section III and discussion in section IV, especially eqs 18 and 19, we know that the parameters from a 10-atom ring structure will be good for AIMs in a very similar molecular environment. When we use this set of parameters for compact structures, some errors are expected. We can assess these errors by calculating the first IE for our model systems shown in Figure 1 using parameters from the 10-atom ring and comparing them with those from SVWN. The difference of the first IE from QEq and SVWN, IE<sub>QEq</sub> – IE<sub>SVWN</sub>, are shown in brackets of Figure 1. For the 10-atom ring itself, the IE from QEq is lower by 0.28 eV which is an error of 4%. For other structures, QEq consistently overestimates the first IE, and for 4 out of 5 structures, the overestimations are around 1 eV. This is consistent with overestimations in previous calculations. Another way to assess the errors is to check the parameters fitted from different model structures. Taking Ag

for example, the coefficients from the 10-atom ring are shown in Table 1. Those from the Ag<sub>12</sub> cuboctahedron, listed starting from the first one, are 4.3306, 3.1165, 0.9682, and 0.9095. When the  $Ag_{12}$  cuboctahedron has a +1 charge, the partial charge on each atom is  $+^{1}/_{12}$  independent of parameters. Because the first and second coefficients from the cuboctahedron fit are lower than those from the 10-atom ring, the IE decreases. The QEq calculations overestimate SVWN IE by 0.78 eV or 12% when using the 10-atom ring parameters and underestimate by 0.19 eV or 3% when using the 12-atom cuboctahedron parameters. We did similar tests on other elements and found the above argument is true for all elements and all model structures we have. As shown in eq 19, all parameters are environment dependent. That is, if atoms of the same element are in different molecular environment in one molecule, they are actually different AIMs. Ideally we should assign different parameters to each of them. We think such a scheme would remove systematic errors. Another advantage of that scheme is that we could estimate charge distributions and dipole moments in pure clusters. However putting this idea into practice is not easy and will require robust automated procedures to derive parameters for AIMs representative of various environments.

#### VI. Conclusion

Based on the analysis and calculations of this study, we can say that the inclusion of third and fourth order terms in the energy expansion eq 1, and use of self-consistent screened Coulomb interactions  $J_{ii}$  in eq 7 eliminate the problem of unphysical atomic charges. It makes QEq more reliable and potentially more accurate. Results for metal dimers and 55-atom alloy clusters<sup>1</sup> show that the QEq ionic contributions to the total energy are essential in mixed metal systems when there are appreciable electronegativity differences between atoms. The IEs of Ag<sub>5</sub>Li<sub>5</sub> and Au<sub>13</sub>Na<sub>n</sub> (n = 1-10) calculated by QEq are surprisingly good, especially in a relative sense (trends). This is important because the IE is one of the easiest property to measure and IEs of metal clusters have been found to correlate with chemical reactivity.<sup>36</sup> More importantly, the analysis in section IV establishes a connection between DFT and the SMP/ OEq approximation. This gives insight into the validity of the approximations and ways to improve them. In particular, we made the assumption, in our current implementation of SMP/ QEq, that the last two terms of eq 14 do not change appreciably when we go from a neutral to a charged system. This may be approximately true in large metal clusters where charging involves the filling or emptying of mostly nonbonding orbitals, but it is clearly a bad approximation in small systems, or covalently bonded systems, where charging occurs via the filling or emptying of bonding and antibonding orbitals. An extreme example of this would be He<sub>2</sub>/He<sub>2</sub><sup>+</sup>/He<sub>2</sub><sup>2+</sup>. Therefore, an important improvement in the future will be to model the chargedependent changes to the covalent energy terms, in both the parametrization and application stages of SMP/QEq.

**Acknowledgment.** This work was made possible by the facilities of the Shared Hierarchical Academic Research Computing Network (SHARCNET:www.sharcnet.ca).

## **References and Notes**

- (1) Zhang, M.; Fournier, R. J. Mol. Struct.: THEOCHEM 2006, 762, 49.
- (2) Cieplak, P.; Cornell, W. D.; Bayly, C.; Kollman, P. A. J. Comput. Chem. 1995, 16, 1357.
  - (3) Sanderson, R. T. Science 1951, 114, 670.

ohio2/yjx-yjx/yjx-yjx/yjx99907/yjx6009d07z	ynnws	23:ver 3	2/26/09	6:17	Msc: in-2008-063273	TEID: crk00	BATID: in4h40
01102/3/2/2/2/2/2/2/2/2/2/2/2/2/2/2/2/2/2/2	Vhhma	20.001.0	2/20/03	0.17	Wisc. jp-2000-000273	I LID. CIKOU	DATID. JP4040

## Self-Consistent Charge Equilibration Method

580

581

582

583

584

585

586

587

588

589

590

591

592

593

594

595

596

597

598

599

600

601

602

603 604

605

606

607

608

610

611

- (4) Sanderson R. T. Chemical Bonds and Bond Energy, 2nd ed.; Academic Press: New York, 1976.
- (5) Mortier, W. J.; Ghosh, S. K.; Shankar, S. J. Am. Chem. Soc. 1986, 108, 4315.
- (6) Mortier, W. J.; Van Genechten, K.; Gasteiger, J. J. Am. Chem. Soc. **1985**, 107, 829.
- (7) Bultinck, P.; Langenaeker, W.; Lahorte, P.; De Proft, F.; Geerlings, P.; Waroquier, M.; Tollenaere, J. P. J. Phys. Chem. A 2002, 106, 7887.
- (8) Bultinck, P.; Langenaeker, W.; Lahorte, P.; De Proft, F.; Geerlings, P.; Waroquier, M.; Tollenaere, J. P.; Van Alsenoy, C.; Tollenaere, J. P. J. Phys. Chem. A 2002, 106, 7895.

  - (9) York, D. M.; Yang, W. J. Chem. Phys. 1996, 104, 159.
    (10) Louwen, J. N.; Vogt, E. T. C. J. Mol. Catal. A 1998, 134, 63.
- (11) Njo, S. L.; Fan, J.; van de Graaf, B. J. Mol. Catal. A 1998, 134,
- (12) Fournier R.; Zhang M.; Soudagar Y.; Hopkinson M. Lecture Series on Computers and Computational Sciences; Simos, T. E., Maroulis, G., Eds.; VSP Brill Academic Publishers: Utreche, The Netherlands, 2005; Vol. 3, p 51.
  - (13) Rappé, A. K.; Goddard, W. A., III. J. Phys. Chem. 1991, 95, 3358.
  - (14) Kitao, O.; Ogawa, T. Mol. Phys. 2003, 101, 3.
- (15) Ogawa, T.; Kitao, O.; Kurita, N.; Sekino, H. Chem-Bio Informat. J. 2003, 3, 78.
- (16) Iczkowski, R. P.; Margrave, J. L. J. Am. Chem. Soc. 1961, 83, 3547.
- (17) Parr R. G.; Yang W. Density-Functional Theory of Atoms and Molecules; Oxford University Press: New York, 1989.
- (18) Cheng, J.; Fournier, R. Theor. Chem. Acc. 2004, 112, 7.
- (19) Nakajima, A.; Hoshino, K.; Naganuma, T.; Watanabe, K.; Kaya, K. Z. Phys. D 1993, 26, S 89.
- (20) Vosko, S. H.; Wilk, L.; Nusair, M. Can. J. Phys. 1980, 58, 1200.
- (21) Hohenberg, P.; Kohn, W. Phys. Rev. B 1964, 136, 864.
- (22) Kohn, W.; Sham, L. J. Phys. Rev. A 1965, 140, 1133.

(23) Slater J. C. Quantum Theory of Molecules and Solids. Vol. 4: The Self-Consistent Field for Molecules and Solids; McGraw-Hill: New York,

J. Phys. Chem. A, Vol. xxx, No. xx, XXXX I

612

613

614

615

616

617

618

619

620

621

622

623

624

625

626

627

628

629

630

631

632

633

634

635

636

637

638

639

640

- (24) Becke, A. D. J. Chem. Phys. 1993, 98, 5648.
- (25) Lee, C.; Yang, W.; Parr, R. G. Phys. Rev. B 1988, 37, 785.
- (26) Becke, A. D. Phys. Rev. A 1988, 38, 3098.
- (27) Perdew, J. P. Phys. Rev. B 1986, 33, 8822.
- (28) Perdew, J. P.; Burke, K.; Ernzerhof, M. Phys. Rev. Lett. 1996, 77,
- (29) Bader R. F. W. Atoms in Molecules. A Quantum Theory; Oxford University Press: New York, 1990.
- (30) Bader, R. F. W.; Nguyen-Dang, T. T. Adv. Quantum Chem. 1981, 14, 63.
- (31) Zhou, X. W.; Wadley, H. N. G. J. Phys.: Condens. Matter 2005, 17, 3619.
- (32) Demiralp, E.; Çagin, T.; Goddard III, W. A. Phys. Rev. Lett. 1999, 82, 1708.
- (33) (a) St-Amant, A.; Salahub, D. R. Chem. Phys. Lett. 1990, 169, 387. (b) St-Amant A. 1992, Ph.D. Thesis, University of Montreal.; Casida M. E.; Daul C.; Goursot A.; Koester A.; Pettersson L. G. M.; Proynov E.; St-Amant A.; Salahub D. R. (principal authors) and Chrétien S.; Duarte H.; Godbout N.; Guan J.; Jamorski C.; Leboeuf M.; Malkin V.; Malkina O.; Nyberg M.; Pedocchi L.; Sim F.; Vela A. (contributing authors) 1998, deMon-KS software version 3.2.
- (34) Andzelm, J.; Radzio, E.; Salahub, D. R. J. Chem. Phys. 1985, 83,
- (35) Bulusu, S.; Wang, L. S.; Zeng, X. C. Proc. Natl. Acad. Sci. 2006, 103, 8326.
  - (36) Knickelbein, M. B. Annu. Rev. Phys. Chem. 1999, 50, 79.

641 JP8063273